

# Effective removal of uranium ions from drinking water using CuO/X zeolite based nanocomposites: effects of nano concentration and cation exchange

M. R. Abdi · H. R. Shakur · Kh. Rezaee Ebrahim Saraee · M. Sadeghi

Received: 1 January 2014 / Published online: 18 April 2014  
© Akadémiai Kiadó, Budapest, Hungary 2014

**Abstract** For the first time, effects of CuO nanoparticles concentration (from 1 to 24.2 wt%) in CuO/NaX nanocomposite and replacing various cations ( $\text{Ag}^+$ ,  $\text{K}^+$ ,  $\text{Ca}^{2+}$ , and  $\text{Mg}^{2+}$ ) with  $\text{Na}^+$  ions in NaX zeolite on removal of uranium ions from drinking water are reported. The removal of uranium was performed under natural conditions of pH, laboratory temperature and the presence of competing cations and anions that are available in tap water of Isfahan city. Characterization of parent NaX zeolite and modified samples were investigated using X-ray fluorescence, X-ray powder diffraction patterns, scanning electron microscopy, and atomic absorption spectroscopy methods. Using Langmuir, Freundlich, and C-models, isotherms of equilibrium adsorption were studied. Results show the removal efficiency and distribution coefficient of NaX zeolite decrease in the presence of other competing anions and cations that exist in drinking water.

But, modification of NaX zeolite with various cations and CuO nanoparticles might enhance the ability of X zeolite in removing uranium from drinking water.

**Keywords** Uranium · Drinking water · CuO/NaX nanocomposite · Ion exchange

## Introduction

Since ancient times uranium has been applied as a colorant in ceramic glazes and then in the glassmaking industry. Today enriched uranium is used in the nuclear industry as fuel elements. Depleted uranium (DU) (the by-product of the enrichment process) is used in the military branches for armour plating and armour piercing ammunition [1]. But, uranium is one of the most dangerous heavy metals in the environment because its chemical toxicity and radioactivity. Uranium contamination poses a threat both to surface and ground waters [2]. Uranium might enter the water from naturally occurring deposits or human activities. Uranium come from mill tailings, emissions from the nuclear industry, combusting coal and other fuels, and phosphate fertilizers that contain uranium [3] and growing use of DU as military munitions [4–6]. The inhalation of uranium compounds results in its deposition in the lungs, which reach kidneys through the blood stream resulting in progressive or irreversible renal injury and in acute cases leading to kidney failure and death. The tolerable daily intake of uranium established by WHO based on Gilman's studies is 0.6  $\mu\text{g}/\text{kg}$  of body weight/day. The WHO, Health Canada, Australian, and USEPA drinking water guidelines fixed the maximum uranium concentration in drinking water should be less than 9, 20, 20 and 30  $\mu\text{g}/\text{L}$  respectively [7].

---

M. R. Abdi (✉)  
Department of Physics, Faculty of Science, University of Isfahan, 81747-73441 Isfahan, Iran  
e-mail: r.abdi@phys.ui.ac.ir

H. R. Shakur · Kh. Rezaee Ebrahim Saraee  
Department of Nuclear Engineering, Faculty of Advance Sciences and Technologies, University of Isfahan, 81746-73441 Isfahan, Iran

H. R. Shakur  
Department of Physics, Faculty of Science, Imam Hossein Comprehensive University, Tehran, Iran

M. Sadeghi  
Department of Chemistry, Faculty of Science, Imam Hossein Comprehensive University, Tehran, Iran

So, the removal of uranium from drinking water is a serious issue. There are several methods for removal of uranium ions from aqueous solutions such as chemical membrane [8], precipitation [9], biological treatment [10], solvent extraction [11], and ion exchange/adsorption [12–15]. But, ion exchange is the most efficient removal method because it might remove about 98 % of uranium from water [16]. Zeolites constitute an important class of aluminosilicate crystalline microporous materials comprising natural and synthetic species. Zeolites represent special physicochemical properties because of their singular structure and have been widely used as molecular sieves, ion-exchangers, absorbents, catalysts, and so on [17–20].

In this research, we have studied the sorption of uranium from tap water of Isfahan city using X zeolites. Parent NaX zeolite was synthesized. To raise the ability of uranium removing from samples, parent zeolite was modified using a coating with CuO nanoparticles with different concentrations and using exchange of various cation ions such as Ag, Mg, Ca, and K studied. Effects of CuO nanoparticles concentration in CuO/NaX nanocomposite and replacing various cations with Na ions in NaX zeolite on removal of uranium in water samples were studied. However to the best of our knowledge, such study there has been not reported in any previous work.

## Experimental

### Synthesis of NaX zeolite

4.2 g  $\text{Al}(\text{OH})_3$  was dissolved in 8.4 mL NaOH aqueous solution (50 % w/v) at 100 °C then 8.5 mL water was added. Then 15.1 g NaOH was added to the mixture and again 60 mL water was added and heated at 50 °C (solution 1). 45.2 g  $\text{Na}_2\text{SiO}_3$  was dissolved by mixing with 250 mL water and 15.2 g NaOH (solution 2). Solutions 1 and 2 were mixed quickly and the final solution was heated at 70 °C in oven. The white powder product washed with water and dried at 80 °C (parent NaX sample).

### Preparation of cation ions exchanged in NaX zeolite

To prepare the exchanged form of NaX, 10 g of the parent zeolite was shaken with 300 mL solution of 1 M  $\text{NH}_4(\text{NO}_3)$  at the 60 °C for 6 h. The solution was decanted and fresh solution was added. This procedure was repeated three times. The solid was filtered, washed and dried at 110 °C. This solid is  $\text{NH}_4$ -form of NaX. The H-form of NaX was prepared by heating the  $\text{NH}_4$ -form at 450 °C for 2 h to remove ammonia molecule. ( $\text{Ag}^+$ ,  $\text{K}^+$ ,  $\text{Ca}^{2+}$ , and  $\text{Mg}^{2+}$ )—exchanged forms that denominated as AgX, KX,

**Table 1** preparation of CuO/NaX samples with different CuO concentration

Samples	$\text{Cu}(\text{NO}_3)_2$ (aq) (M)	CuO loading (wt%)
CuO/NaX 1	0.01	1.0
CuO/NaX 2	0.05	6.8
CuO/NaX 3	0.1	8.4
CuO/NaX 4	0.2	9.7
CuO/NaX 5	0.5	12.5
CuO/NaX 6	1	24.2

**Table 2** Various parameters of drinking water of Isfahan city

Parameter	Unit	Value
PH	–	7.63
Total dissolved solids	mg/L	250
Turbidity	NTU	0.6
Hardness	mg/L	166.5
Conductivity	$\mu\text{S}/\text{Cm}$	393
Methylorange basicity	mg/L	130
Aluminium	mg/L	0.08
Lead	mg/L	0.00261
Zinc	mg/L	<0.04
Chloride	mg/L	23.04
Fluoride	mg/L	0.15
Sulfate	mg/L	35.32
Nitrate	mg/L	8.72
Magnesium	mg/L	17.99
Sodium	mg/L	15.7
Potassium	mg/L	0.81
Calcium	mg/L	37.07
Bicarbonate	mg/L	158.6
Uranium	ppb	< 20

CaX, and MgX zeolites were prepared by shaking 2.5 g of an H-form of zeolite with 100 mL of 0.1 M solution of  $\text{AgNO}_3$ ,  $\text{KNO}_3$ ,  $\text{Ca}(\text{NO}_3)_2$  and  $\text{Mg}(\text{NO}_3)_2$  at 60 °C for 24 h respectively. For each sample, the solution was decanted and fresh solution was added. This procedure was repeated three times. The solid was separated, washed with distilled water, dried at 110 °C overnight, and stored in the desiccator until use.

### Preparation of CuO/NaX nanocomposite

The samples of CuO/NaX with different CuO concentrations were synthesized:  $\text{Cu}(\text{NO}_3)_2$  solutions with different molarities (Table 1) were prepared at first, then 1 g NaX powder was added into each solution meanwhile the suspension was stirred strongly at ambient temperature for

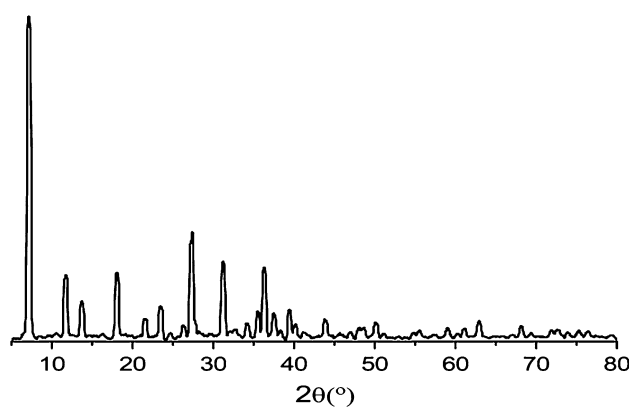


**Fig. 1** XRD pattern of synthesized NaX zeolite

6 h. The green powders were filtered, washed with distilled water and dried overnight at 110 °C. The obtained products were calcined at 500 °C in the air for 6 h [21].

#### Uranium removal from tap water

1,000 mL of drinking water of Isfahan (tap water) was analyzed (Table 2). The standard uranium feed solution was prepared by dissolving a proper quantity of uranyl nitrate hexahydrate ( $\text{UO}_2(\text{NO}_3)_2 \cdot 6\text{H}_2\text{O}$ ) in 500 mL of this water.

The working solutions were prepared from the stock solution. Batch experiments using the aforementioned solutions were done at laboratory temperature by stirring of a 20 mL uranium solution with 0.2 g of the added absorbent. No additional operations for adjusting of the pH were done.

#### Characterization

Synthesized materials were characterized using different techniques of X-ray diffraction (XRD) (Bruker, D8ADVANCE) with  $\text{Cu-K}_\alpha$  radiation, X-ray fluorescence (XRF) (Bruker, S4 PIONEER), scanning electron microscopy (SEM) (TESCAN, VEGA II). The concentration of uranium in solutions was measured by inductively coupled plasma atomic emission spectroscopy. The amount of copper in the samples was measured using an atomic absorption spectrometer (AAS) (Shimadzu, AA 470).

## Results and discussion

#### Characterization of samples

Figure 1 shows the XRD pattern of the synthetic parent NaX sample. In this figure the characteristic peaks at  $2\theta$

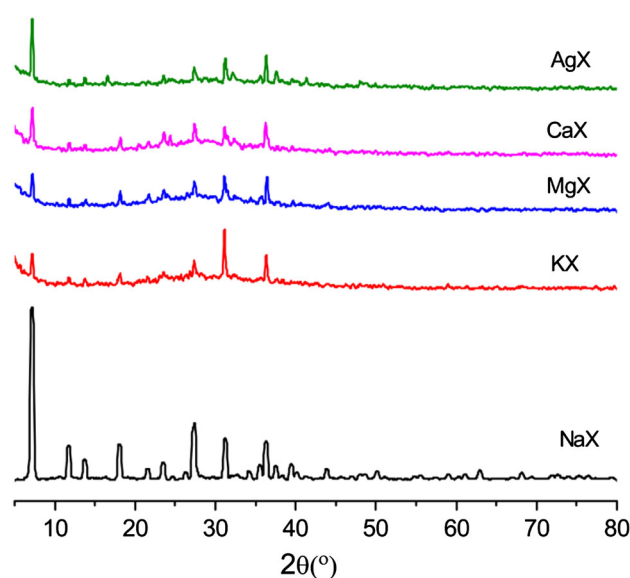


**Fig. 2** XRD patterns of parent NaX zeolite and ion exchange modified parent NaX zeolite

values of 7.054, 11.615, 13.447, 17.930, 21.435, 23.335, 26.17, 27.08, 27.827, 31.068, 31.880, 34.062, 35.351, 36.178, 37.357, 39.254, 39.973, 41.120, 43.650, 45.336, 47.888, and 48.449° are corresponded to the Miller indices (h k l) of (1 1 1), (2 2 0), (3 1 1), (3 3 1), (5 1 1), (4 4 0), (6 2 0), (5 3 3), (6 2 2), (6 4 2), (7 3 1), (7 3 3), (6 6 0), (5 5 5), (4 8 0), (6 6 4), (9 3 1), (8 4 4), (10 2 2), (8 6 4), (8 8 0), and (9 5 5) respectively that are in good agreement with those of the Face-centered cubic crystal structures of NaX zeolite (molecular formula:  $\text{C}_5\text{H}_4\text{O}_2 \cdot \text{Na}_2\text{O} \cdot \text{Al}_2\text{O}_3 \cdot 3.3\text{SiO}_2 \cdot 7\text{H}_2\text{O}$ ) with lattice parameter of  $a = 24.96000 \text{ \AA}$  (pdf No. 41-118).

XRD patterns of AgX, KX, MgX, and CaX zeolites are shown in Fig. 2. This figure shows that the structures of these zeolites are retained even after the metal cation exchange. This indicates the absence of any structural damage of NaX zeolite during ion exchange and calcination processes.

However, the XRD patterns of the metal ions exchanged zeolite showed lowering of the peak intensity. This observed decrease could be caused by structural deformation occurring during exchange of  $\text{Ag}^+$ ,  $\text{K}^+$ ,  $\text{Ca}^{2+}$ , and  $\text{Mg}^{2+}$  cations into the zeolite structure or interaction of these cations with the framework oxygen of zeolite [22]. The region at  $2\theta$  values among 10° and 20° have been considered to be correlated with the locations of cations in the zeolite framework. From all zeolites one can see the reduction of the characteristic peaks, indicating a redistribution of intra zeolite charge balancing cations [23].

Major element compositions of the parent NaX zeolite and other exchanged form samples that determined by XRF

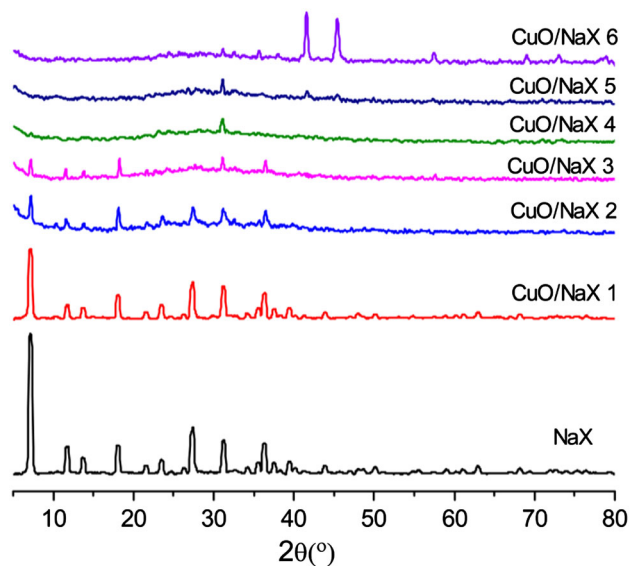
**Table 3** Elemental analysis of parent NaX zeolite and CaX, KX, AgX, and MgX zeolites

Compound	Concentration (wt%)				
	NaX	CaX	MgX	AgX	KX
SiO <sub>2</sub>	47.04	50.08	51.31	41.99	50.12
Al <sub>2</sub> O <sub>3</sub>	30.55	34.11	33.83	28.51	33.88
Na <sub>2</sub> O	9.51	1.28	1.54	0.351	1.19
SO <sub>3</sub>	0.673	0.042	0.046	–	0.050
K <sub>2</sub> O	0.574	0.274	0.285	0.175	5.63
Fe <sub>2</sub> O <sub>3</sub>	0.509	0.521	0.551	0.541	0.540
CaO	0.128	2.97	0.432	0.099	0.125
TiO <sub>2</sub>	0.035	0.037	0.041	0.039	0.042
Cl	0.034	0.016	0.016	0.035	–
CuO	0.015	0.013	0.013	0.029	0.012
P <sub>2</sub> O <sub>5</sub>	–	0.015	0.022	–	0.015
BaO	–	0.021	0.022	–	0.022
ZnO	–	0.005	0.007	0.014	0.008
Cr <sub>2</sub> O <sub>3</sub>	–	–	–	0.013	–
AgO	–	–	–	19.46	–
MnO	–	–	0.021	–	–
MgO	–	–	0.855	–	–
LOI <sup>a</sup>	10.77	10.58	11.01	8.75	8.36
Total	99.84	99.96	100.00	100.00	99.99

<sup>a</sup> Loss on ignition (1000 °C, 2 h)

analysis are summarized in Table 3. These data show that interested elements (Ca, K, Mg, and Ag) replaced in the parent zeolite during the ion exchange process in each sample. The important parameter that determines the ability of zeolites as an efficient absorbent material is a Si/Al ratio. This parameter has a value below 1.6 in all samples.

The copper in the CuO/NaX nanocomposites was measured using an AAS and results are shown in Table 1. Figure 3 shows the XRD patterns of the CuO/NaX nanocomposites with different CuO nanoparticles concentration from 1 to 24.2 wt%. This figure indicates that the structure of zeolites remains intact after loading low CuO over NaX. No peak of copper oxide founded on CuO loaded material upto 9.7 wt% which indicated that in low CuO concentration samples there was no new phase formation during heat treatment and CuO loading. This confirms that copper oxide in porous NaX might automatically be dispersed [24]. CuO nanoparticles are included inside the channels of the zeolite and are too small to give the corresponding diffraction pattern. Depending on CuO contents the intensities of some peaks were varied. The higher intensity was observed in the parent zeolite. The intensities of some diffraction peaks decrease or disappear with a raise of CuO loading. The decrease in the intensities might be because of

**Fig. 3** XRD patterns of parent NaX zeolite and CuO/NaX nanocomposites

the high absorption coefficient of CuO nanoparticles. Diffraction peaks of CuO nanoparticles could be observed for samples with above 9.7 wt% CuO. In these cases, it is believed that CuO nanoparticles have grown on the external surface of the zeolites and covered the entire surface with them [25, 26].

The spectra of these samples show three broad peaks at  $2\theta$  37.949, 45.294, and 54.336 positions. These peaks are in good agreement with those of the monoclinic crystal structures of CuO (Tenorite), which were consistent with values of standard card (pdf No. 5-661).

The three diffraction peaks correspond to (1 1 0), (1 1 1), and (–1 1 0) planes, respectively. The broadening of XRD lines is attributed to nanocrystalline characteristics of the sample, which indicates that the particle sizes are in the nanometer range.

From the width of the XRD peak ( $\beta$ ) broadening ((1 1 0) plan), the average crystalline size has been calculated using Scherer's equation [27]:

$$D = \frac{K\lambda}{\beta \cos \theta} \quad (1)$$

where  $D$  is the diameter of the particles,  $K$  is a geometric factor taken to be 0.9,  $\lambda$  is the X-ray wavelength,  $\theta$  is the diffraction angle and  $\beta$  is the full width at half maximum of the diffraction peak at  $2\theta$ . The mean crystal size of CuO particles resulted to be 30 nm.

In Fig. 4 SEM images of samples are given. Comparison of NaX zeolite morphology with AgX zeolite and CuO/NaX nanocomposite shows that cubic morphology and crystallite size are retained on samples.

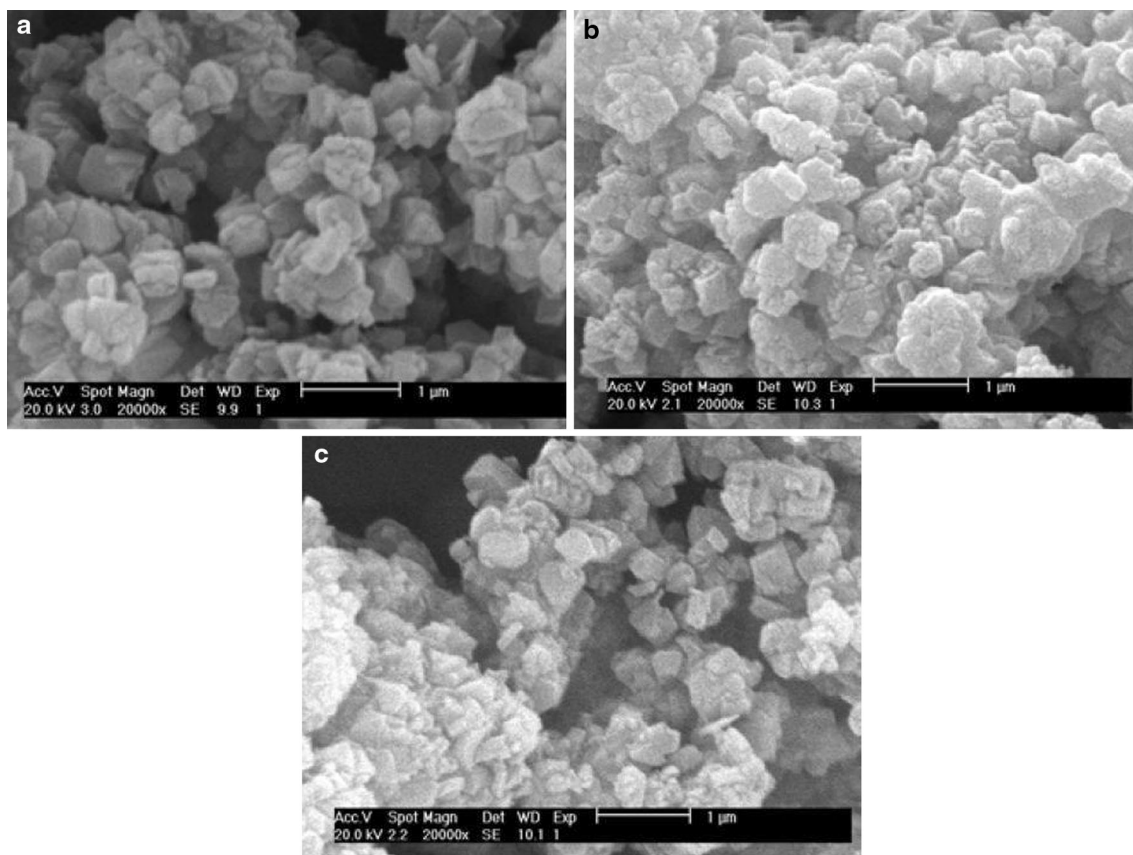


**Fig. 4** SEM images of **a** NaX, **b** AgX, and **c** CuO/NaX zeolites

**Adsorption experiments**

The effects of various parameters such as initial uranium concentration, cation ion exchange, and CuO nanoparticles concentration were investigated. The effects of contact time on the adsorption of uranium ions on NaX zeolite which studied by Olguin and et al. [19] and Akyil and et al. [20] show that equilibrium was gained before 15 min. Hence, in all experiments, contact time was chosen as 1 h.

The removal efficiency was calculated using the following equation [28]:

$$R(\%) = \frac{(c_0 - c_e)}{c_0} \times 100 \tag{2}$$

where  $C_0$  and  $C_e$  are the uranium ion concentrations in the aqueous phase before and after sorption.

Amount of uranium adsorbed per unit mass of NaX zeolite at equilibrium was calculated according to fallowing equation [29]:

$$q_e(\text{mg/g}) = (C_0 - C_e) \frac{v}{m} \tag{3}$$

where  $v$  is the batch volume (L) and  $m$  is the adsorbent mass(g).

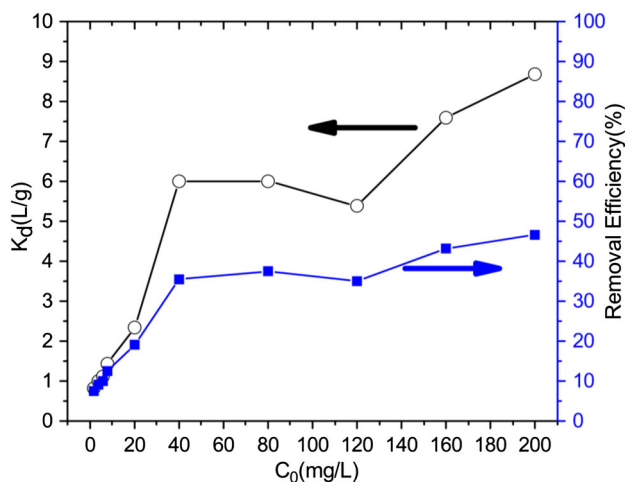


**Fig. 5** Removal efficiency and distribution coefficient (must be multiplied by  $10^{-2}$ ) of uranium on the parent NaX zeolite

The distribution coefficient  $K_d$  is defined as the ratio of the concentration of the uranium in the sorbent and in the solution at equilibrium [30]:

$$K_d(\text{L/g}) = \frac{q_e}{C_e} \tag{4}$$

### Effect of uranium concentration

One of the most important parameter which can influence the sorption behavior of uranium is the initial uranium concentration. By calculating the distribution coefficient and the removal efficiency at different initial concentrations, the effect of initial concentration on the adsorption of uranium by NaX zeolite was studied. Variations of removal efficiency and distribution coefficient as a function of initial uranium concentration from 2 to 200 mg/L are shown in Fig. 5.

It is clear that removal efficiency and distribution coefficient raise with increasing initial uranium concentration in the solution. In higher uranium concentration solutions, uranium ions have more chance to adsorb onto active sites of zeolite in the presence of other competing cations and anions in tap water which listed in Table 2. Upto 40 mg/L initial uranium concentration, removal efficiency rapidly raises and then smoothly increases.

This might be due to saturation of active sites available for uranium adsorption, and the presence of competing cations and anions, that significantly affect the uranium adsorption process. On the other hand, removal efficiency and distribution coefficient of NaX zeolite generally are reduced in the presence of other competing ions available in tap water [19, 20].

### Adsorption isotherms

The adsorption isotherms were studied by analyzing solutions in contact with parent NaX zeolite before and after equilibrium. The sorption isotherms were studied at tap water normal pH, laboratory temperature (28–30 °C), and initial solution concentrations from 2 to 200 mg/L.

Freundlich isotherm is used for modeling the adsorption on heterogeneous surfaces. It suggests that sorption is not restricted to one specific class of the sites and assumes surface heterogeneity. This isotherm can be explained by the following equation [31]:

$$q_e = K_F C_e^{1/n} \quad (5)$$

where  $K_f$  (mg/g) and  $n$  are constant.

Langmuir isotherm models the single coating layer on adsorption surface. This model supposes that the adsorption takes place at a specific adsorption surface. The attraction between molecules decreases as they are getting further from the adsorption surface. Langmuir isotherm can be defined according to the following equation [32]:

$$q_e = \frac{K_a q_m C_e}{1 + K_a C_e} \quad (6)$$

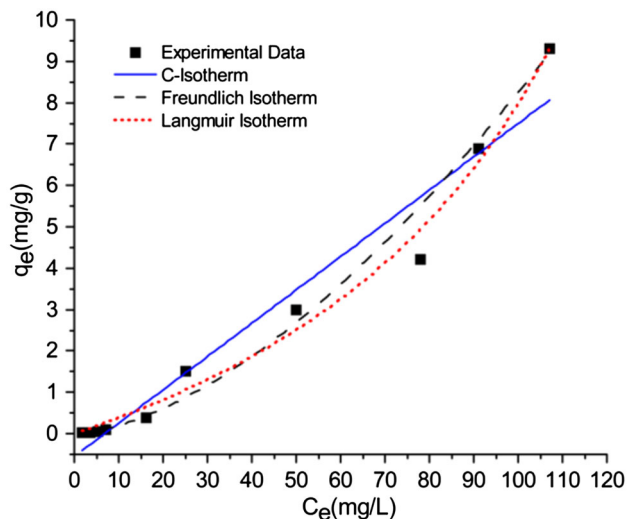


Fig. 6 Sorption isotherms of U ions on NaX zeolite

where  $K_a$  (L/mg) and  $q_m$  (mg/g) are Langmuir constant and maximum monolayer adsorption capacity respectively.

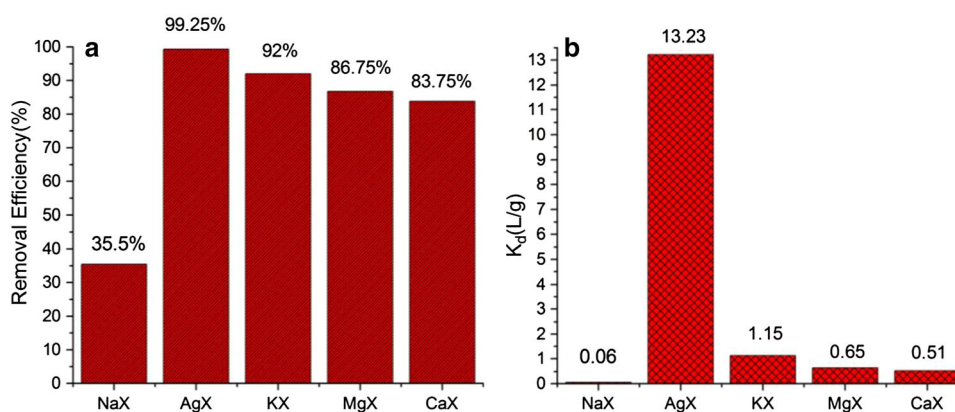
Also, the C-isotherm was tested. In this model, ratio between the concentration of the compound remaining in solution and adsorbed on the solid is the same at any concentration. This ratio is usually named distribution coefficient or  $K_d$  (L/g) [33]. The C-isotherm can be expressed by the following equation:

$$q_e = K_d \times C_e \quad (7)$$

Figure 6 shows the plots of Freundlich, Langmuir, and C models. The sorption constants of these three models and their correlation coefficients ( $R^2$ ) were calculated and presented in Table 4. Due to negative slope and intercept, the experimental data from Table 4 did not fit to the Langmuir isotherm. Therefore, the adsorption behavior of the tested system does not follow the assumption on which the Langmuir approach is based. Also, the experimental data did not fit to the Freundlich isotherm properly. The calculated value of  $n$  for Freundlich isotherm from Table 4 is lower than 1. Reed and Matsumoto [34] have pointed out that the situation  $n > 1$  is most common and may be due to a distribution of surface sites or any factor that cause a decrease in adsorbent–adsorbate interaction with increasing surface density. According to McKay et al. [35] the values of  $n$  in the range of 2–10 represent good adsorption [36]. However, the C-isotherm plot shows good fit to the experimental adsorption data with relatively high correlation coefficients ( $R^2 = 0.9479$ ), which supports that the adsorption of uranium ions onto NaX zeolite follows the C-isotherm. The  $K_d$  calculated from the slope of the regression line is 0.08045 L/g which is in good agreement with actual average experimental distribution coefficient (0.06 L/g) for NaX. Because the tolerance of the

**Table 4** Various adsorption isotherm model parameters

Isotherm Parameter	Freundlich isotherm		Langmuir isotherm		C-isotherm
	$K_F$	$1/n$	$q_m$	$K_a$	$K_d$
Value	$0.00386 \pm 0.00344$	$1.65724 \pm 0.19637$	$-6.77177 \pm 1.4473$	$-0.00541 \pm 5.408E-4$	$0.08045 \pm 0.00627$
$R^2$	0.9767		0.98588		0.9479

**Fig. 7** **a** Removal efficiencies and **b** distribution coefficients of uranium on NaX, AgX, KX, CaX, and MgX zeolites

experimental data, the curve of C-isotherm is not a line of zero-origin and has an intercept with  $-0.54881$  value.

#### Effect of cation exchange

The removal efficiency and distribution coefficient for the adsorption of uranium ions of silver, potassium, magnesium, and calcium exchanged forms of NaX zeolite have been determined and shown in Fig. 7.

The differences in the adsorption properties of various kinds of X zeolite might be understood in terms of their framework structure and the location of the cations that balance the charges on the zeolite framework. The uranium (VI) species with the smallest ionic radius that occurs in the aqueous solution is the uranyl ion,  $UO_2^{2+}$ , which is present in aqueous solutions in its hydrated state [16]. The radius of the hydrated uranyl cation is comparable with pore size of NaX zeolite. On the other hand, the surface area and pore volume of the NaX decrease of univalent ion ( $Ag^+$  and  $K^+$ ) exchanged forms because the size of  $Ag^+$  and  $K^+$  ions is more than exchangeable sodium cation. Therefore, the radius of hydrated uranyl cation is greater than the mean dimension of the zeolite channels indicating that the U (VI) species in the solution have no access to the exchangeable sites of the AgX and KX zeolites.

However, positively and negatively charged sites exist on the surface of the zeolite. These charged sites are directly accessible to uranium ions present in aqueous solutions and thus can contribute to uranium removal from the solution through a typical adsorption mechanism [14].

Therefore the major interaction of uranium ions with AgX and KX zeolites is electrostatic interaction which is directly proportional to charge density of cations.  $Ag^+$  and  $K^+$  cations have a lower charge density than  $Na^+$  which causes decreased the repulsion and raising the attraction electrostatic forces between uranium ions and zeolite surface (improve basicity). Ionic radius of  $K^+$  is larger than  $Ag^+$  which causes its lower charge density. But in AgX zeolite, the weight percent of silver is 19.46 % whereas in KX zeolite weight percent of potassium is only 5.63 % (Table 3) which caused the removal parameters of AgX zeolite are more than KX zeolite.

When divalent cations ( $Mg^{2+}$ ,  $Ca^{2+}$ ) replaced with sodium ions in NaX zeolite, one divalent cation replaces two sodium ions; therefore, half the cations are present in the framework of zeolite. This causes an enhancement in basicity of zeolite which led to an increasing in removal efficiency and distribution coefficient in MgX and CaX zeolites compared with NaX zeolite [22, 37–39].

#### Effect of CuO nanoparticles concentration

CuO is a semiconductor which has been widely used as a photocatalyst, catalyst for the oxidation of alcohols and aromatic hydrocarbons, and removal of heavy metals from aqueous solutions. In this study CuO/NaX nanocomposite is used for removal of uranium ions from tap water. Effects of various concentrations of CuO nanoparticles on removal efficiency and distribution coefficient were investigated and are shown in Fig. 8. As in this figure, removal

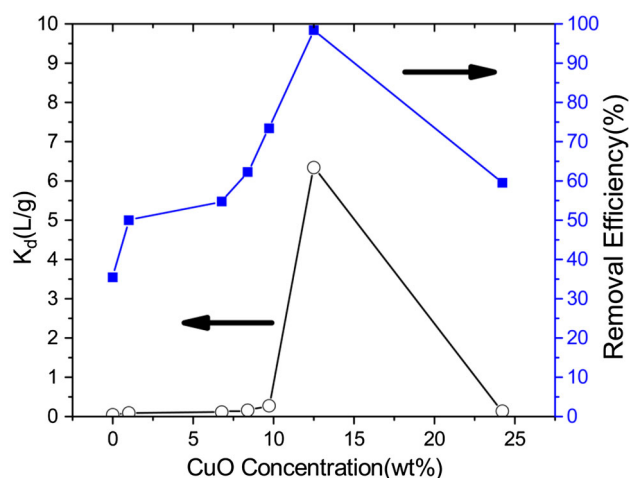


**Fig. 8** Effects of CuO nanoparticles concentration on removal efficiency and distribution coefficient of uranium on CuO/NaX nanocomposite

efficiency and distribution coefficient raise by increasing the CuO concentration up 12.5 wt% and then drop off. All zeolites have acidity in Bronsted and Lewis acid sites. It has been reported that the Bronsted/Lewis ratio decreases with the loading of CuO on zeolites. Because the acidity strength of Lewis acid sites is weaker than that of Bronsted acid sites, the acidity strength of zeolites is weakened when CuO nanoparticles are added to them [21, 39, 40]. Reduction in the acidity strength of CuO/NaX absorbent led to increase the electrostatic interaction between the uranium cations in solution and surface the absorbent. Both capabilities of CuO nanoparticles [41] and NaX zeolite provide a dual active sites system for removal of uranium ions from tap water. Therefore with increasing the concentration of CuO nanoparticles removal efficiency and distribution coefficient increase as shown in Fig. 8. However in sample with above 12.5 wt% CuO concentration, the zeolite structure was collapsing and then only CuO phase was existed which causes a reduction in removal efficiency and distribution coefficient of absorbent.

## Conclusion

NaX zeolite and silver, potassium, magnesium, and calcium exchanged forms of NaX zeolite, and CuO/NaX nanocomposite synthesized and used for removal of uranium ions from drinking water of Isfahan city. Results show that although removal properties such as removal efficiency and distribution coefficient of parent NaX zeolite were decreased in the presence of other competing anions and cations which exist in tap water but modification of parent NaX zeolite with various cations through ion

exchange method and loading of CuO nanoparticles over parent NaX zeolite can significantly enhance the ability of NaX zeolite for removal of uranium ions from tap water.

## References

1. Stalder E, Blanc A, Haldimann M, Dudler V (2012) *Chemosphere* 86:672–679
2. Kumar S, Loganathan VA, Gupta RB, Barnett MO (2011) *J Environ Manag* 92:2504–2512
3. Birke M, Rauch U, Lorenz H, Kringel R (2010) *J Geochem Explor* 107:272–282
4. Nriagu J, Nam DH, Ayanwola TA, Dinh H, Erdenechimeg E, Ochir C, Bolorma TA (2012) *Sci Total Environ* 414:722–726
5. Carvalho FP, Oliveira JM (2010) *Environ Int* 36:352–360
6. Sidhu SH, Keith-Roach MJ, Lloyd JR, Vaughan DJ (2010) *Sci Total Environ* 408:5690–5700
7. Milja TE, Prathish KP, Rao TP (2011) *J Hazard Mater* 188: 384–390
8. Fathizadeh M, Aroujalian A, Raisi A (2011) *J Membr Sci* 375:88–95
9. Aydin FA, Soylak M (2007) *Talanta* 72:187–192
10. Shinde NR, Bankar AV, Kumar AR, Zinjarde SS (2012) *J Environ Manag* 102:115–124
11. Agrawal YK, Shrivastav P, Menon SK (2000) *Sep Purif Technol* 200:177–183
12. Fan FL, Qin Z, Bai J, Rong WD, Fan FY, Tian W, Lei XW, Wang Y, Zhao L (2012) *J Environ Radioact* 106:40–46
13. Nilchi A, Shariati Dehaghan T, Rasouli Garmarodi S (2013) *Desalination* 321:67–71
14. Krestou A, Xenidis A, Panias D (2003) *Miner Eng* 16:1363–1370
15. Baybas D, Ulusoy U (2011) *J Hazard Mater* 187:241–249
16. Mar Camachoa L, Denga S, Parra RR (2010) *J Hazard Mater* 75:393–398
17. Weihua Z, Lei Z, Rungping H (2009) *Chin J Chem Eng* 17(4):585–593
18. Kilincarslan Kaygun A, Akyil S (2007) *J Hazard Mater* 147:357–362
19. Olguin MT, Solache-Rios M, Acosta D, Bosch P, Bulbulian S (1999) *Micropor Mesopor Mater* 28:377–385
20. Akyil S, Aslani MAA, Aytas SO (1998) *J Alloy Compd* 271/273:769–773
21. Aboul-Fotouh SMK, Hassan MMI (2010) *Acta Chim Slov* 57:872–879
22. Sebastian J, Mohan Jinka K, Vir Jasra R (2006) *J Catal* 244: 208–218
23. Schwartzberg AM, Zhang JZ (2008) *J Phys Chem C* 112: 10323–10337
24. Zaidi HA, Pant KK (2005) *Can J Chem Eng* 83:970–977
25. Bouvy C, Marine W, Sporken R, Su BL (2007) *Colloid Surf A* 300:145–149
26. Huang M, Xu C, Wu Z, Huang Y, Lin J, Wu J (2008) *Dyes Pigments* 77:327–334
27. Shakur HR (2011) *Physica E* 44:641–646
28. Singh BK, Tomar R, Tomar R, Tomar SS (2011) *Micropor Mesopor Mater* 142:629–640
29. Hernández-Montoya V, Pérez-Cruz MA, Mendoza-Castillo DI, Moreno-Virgen MR, Bonilla-Petriciolet A (2013) *J Environ Manag* 116:213–221
30. Taffarel SR, Rubio J (2010) *Miner Eng* 23:1131–1138
31. Shaheen SM, Eissa FI, Ghanem KM, Gamal El-Din HM, Al Anany FS (2013) *J Environ Manag* 128:514–521

32. Kumar Jha V, Nagae M, Matsuda M, Miyake M (2009) *J Environ Manag* 90:2507–2514
33. Limousin G, Gaudet JP, Charlet L, Szenknect S, Barthes V, Krimissa M (2007) *Appl Geochem* 22:249–275
34. Reed BE, Matsumoto MR (1993) *Sep Sci Technol* 28:2179–2195
35. McKay G, Otterburn MS, Sweeney AG (1981) *Water Res* 14:14–20
36. Ozer A, Pirincci HB (2006) *J Hazard Mater B* 137:849–855
37. Jie Y, Dinghua Y, Peng S, He H (2011) *Chin J Catal* 32(3): 405–411
38. Zhang J, Singh R, Webley PA (2008) *Micropor Mesopor Mater* 111:478–487
39. Kovacheva P, Arishtirova K, Vassilev S (2001) *Appl Catal A Gen* 210:391–395
40. Huang Q, Xue X, Zhou R (2011) *J Mol Catal A* 344:74–82
41. Mahdavi S, Jalali M, Afkhami A (2012) *J Nanopart Res* 14:846–864